In recent years, Navy Navigational Satellites have been operating at temperatures some 20° to 30°F higher than were predicted from preflight tests and calculations. Therefore, an exhaustive analysis of the thermal design was conducted, which was followed by a very extensive thermal vacuum testing program to aid in correcting this situation. The testing program verified most of the analysis and supplied answers to problems that could not be answered in the analysis. As a result of both the analysis and the testing program, the difference between orbital results and preflight calculations has been reduced to a range of from 2° to 3°F.

S. E. Willis, Jr.

THERMAL

For the past two years, signals transmitted by orbiting satellites developed by the Applied Physics Laboratory have provided the Navy with an accurate, world-wide navigational system. However, realizing that such a system is never completely perfected, APL has sought to achieve improved satellite performance and to extend the useful life of the satellites' electronic equipment. These objectives were found to be attainable if the interior temperature of the individual satellites could be maintained at a constant and mild level.

The operating temperature of a satellite is determined by the balance between the internally generated power, the externally absorbed power from the sun and the earth, and the rate at which heat is emitted from the satellite to free space. The balance is a delicate one—a change of 5% in the absorbed power level would cause the internal temperature of the satellite to change by 15° to 20°F, and a change of 5% in internal power dissipation would cause the internal temperatures to change by 6° to 8°F.

The direct solar input is generally the largest heat source. As the earth rotates about the sun, the angle between the earth-sun line and the plane of the satellite's orbit changes, causing the fraction of time the satellite spends in the earth's shadow to vary. Although the thermal capacity of the satellite is generally sufficient to keep the internal temperature from changing more than 2° to 4°F during a single orbit, the total heat absorbed in a minimum-sunlight orbit is 70% or less of that which is absorbed when the satellite is illuminated all of the

DESIGN of CURRENT NAVIGATIONAL SATELLITES

time. The variation in the intensity of the sunlight caused by the seasonal variation in the distance from the earth to sun and the increase in the amount of heat absorbed over the useful life of the satellite caused by degradation of the exterior paint with utraviolet degradation combine to cause an additional variation of 40% to 50% in the amount of heat absorbed from the sun.

It is clear then that the desired narrow band of acceptable operating temperatures cannot be achieved by passive means. Accordingly, a thermostatically controlled heating system was devised. The individual resistive heaters attached to the components are powered by the solar array and controlled by mercury thermostats. The goal of the thermal design is to use available amounts of solar array power in the coldest case and almost none in the hot case to maintain the critical satellite components in the range of 60° to 70°F.

Data are now being received from satellites with this automatic temperature control (ATC) system design, which indicates they are performing very well. The difference between prelaunch predictions of temperatures and the temperatures actually achieved in orbit is much less than for any other satellites designed at APL. The critical components, which are the power system batteries, their associated zener diodes, and the electronic "book" packages, have been held between 63° and 73°F—a range that should extend the life of the memory and power systems. This article describes the methods of designing the heat flow system to achieve these results.

The thermal design of a satellite involves design

of the external paint scheme, the provision of sufficient heating capacity, and the design of suitable heat transfer paths to utilize efficiently the available automatic temperature control power. To minimize solar heating, the satellite body was painted white. For precise temperature control it was decided that heaters with individual thermostats would be placed directly on each of the components requiring constant temperature. This called for 16 heating units for each satellite. The conductive heat flow paths were controlled by the proper selections of spacer materials between the inner and outer structures. The radiative heat flow paths were controlled by the selection of the number of layers of aluminized mylar between the inner components and the outer structure.

Heat Sources

The internally generated heat of the satellite consists of heat generated by the electronics and the thermostatically controlled heater output. The heat sink is the exterior of the satellite.

The major contributors of heat are the oscillator, located in the thermally isolated center structure of the satellite; the electronic "books," located in four quadrants around the center structure; the power system batteries, located between the book quadrants; and the transmitters and voltage regulator, mounted on the bottom or baseplate of the satellite.

The heat output of the oscillator is nearly constant. The outside temperature of the oscillator is not critical since satisfactory operation is attained over a range of 50° to 120°F.

The book heat dissipation is nearly constant, but most effective operation is attained when the temperature variation is only 10° to 15°F.

The battery heat output is the most unpredictable, and the temperature requirements are the most critical of any in the satellite. The heat output is influenced by battery efficiency and therefore by battery temperature, and by the charging cycle. This charging cycle is influenced by the portion of time per orbit that the satellite is in the earth's shadow; by the seasonal variation in the intensity of the sun; by the azimuth angle of the solar blades relative to the plane of the orbit; and by the degradation of the solar cells on the solar blades.

The dissipation of the transmitters is approximately constant, and that of the voltage regulator is dependent upon the power system. However, the *allowable* operating temperature *range* of the transmitters and voltage regulator is very wide so that the only effect of variations in voltage regulator dissipation is the effect that it has on the temperature of the baseplate.

The heating units are controlled by mercury thermostats that close when the temperature is below 70°F and open when the temperature is above 70°F.

Heat Transfer Paths

Heat is transferred between components and from the interior to the exterior of the satellite by both radiation and conduction and is dissipated from the external surfaces by radiation into space. Paths for heat flow exist through the electronic components themselves and through their supporting structures. Detailed methods of solving for resistance to heat flow are given in the following sections. Where it was not possible to determine resistances analytically, vacuum thermal mock-up tests were conducted.

Heat flow paths are dictated by the structure of the satellite; however, several paths can be varied by the designer to provide the desired temperature control. Figure 1 is a schematic diagram which shows the thermal paths in the satellite between the various heat sources and the outside shell. The thermal resistances shown in the shaded areas in Fig. 1 are made of suitable material. Where highly conductive paths are desired, soft aluminum slugs are used. For higher thermal resistance, G-10 epoglass is used. In addition, the depth of multilayer thermal insulation between the inner structure and the outer shell can be adjusted to meet heat flow requirements. The general philosophy adopted was to make the conductive resistances as low as possible and to control the overall internal to external resistance with the number of layers in the multilayer radiation insulation blanket.

Optimum values of the resistances could not be determined directly. Numerous vacuum thermal mock-up tests were not advisable although this method could be used to check the design. A practical method had to be devised to determine the values of the variable resistances, which would provide satisfactory temperature control under all possible orbit conditions. An electrical analog of the heat-flow system was therefore constructed, using values for the heat transfer paths determined as described below. The model was corrected and refined in accordance with results from vacuum thermal mock-up tests. The best values for the variable resistances could then be determined by using the model to simulate all possible conditions of satellite orbit.

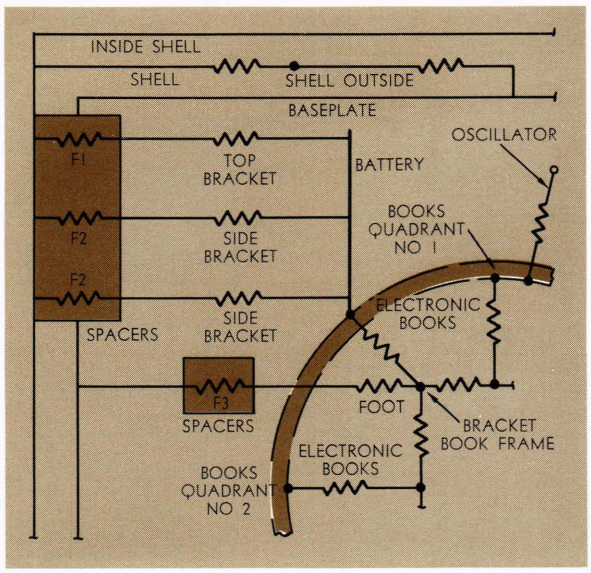

Fig. 1—Schematic diagram showing basic thermal conduction paths, within satellite. (Only one quadrant of the satellite is shown.)

Conduction Paths

The basic thermal conduction paths of the satellite are shown in Fig. 1. The values of the thermal resistances with the exception of F1, F2, and F3, were more or less dictated by structural considerations. The uncertain resistance between members was greatly reduced by using silicone grease, indium foil, and as many fasteners as practical. Still the assumption of zero thermal resistance across the joints caused the analysis to be slightly in error when compared to thermal vacuum tests of the satellites.

The thermal resistance of the connections F1, F2, and F3 between the satellite interior and exterior which consist of spacer material in parallel with metallic screws, could be selected at will. The F3 resistances provide the path for dissipation of internal power through the "baseplate." The F1 and F2 resistances link the various parts of the internal structure to the "shell." To achieve the design goal of using all available automatic temperature control power in the cold case, it was necessary to make the F1 and F2 spacers as conductive as possible. This and the use of low radiation resistance material also allowed the satellite to operate at the desired temperatures in the cases where the exterior was hot. The use of soft aluminum as spacer material provided a satisfactorily low resistance as was verified by later analog tests.

The baseplate is the metallic plate on the bottom of the satellite body where the satellite is mounted to the rocket during launch. The shell is that portion of the satellite body consisting of the top, side, and the epo-glass portion of the bottom.

Fortunately, all of the internal structural members were formed from sheet metal with approximately constant cross-section. It was therefore possible to construct an electrical analog of the thermal situation by cutting analogous blank patterns out of teledeltos paper, an electrically conductive material commonly used in analog field plotter work. Heat which is conducted from one isothermal area (a node) to another is exactly analogous to an electrical charge which is conducted from one equipotential area to another. If the shapes and contact areas of the teledeltos paper duplicate those of the sheet metal the electrical resistances of the paper will simulate exactly the thermal resistances of the metal.

It was not possible to obtain analytically the conductive or radiative resistance between shell and baseplate or that between the inside and the outside of the shell. These resistances were obtained during thermal vacuum testing of a thermal mock-up of the satellite as discussed below.

To simplify the conductive and radiative resistance diagram, two important assumptions were made.

1. The temperature of each of the four battery stacks is equal to the average battery temperature.
2. The temperature of each of the four book quadrants is equal to the average book temperature.

With the use of these assumptions and the customary Δ-Y network transformations, the network of Fig. 1 reduces to that of Fig. 2.

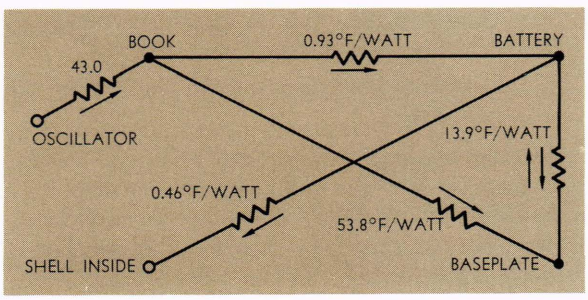

Fig. 2—Reduced conductive paths.

Internal Radiative Paths

The radiation heat transfer paths were of necessity evaluated by two different methods. It was possible to use a standard analysis to determine the radiation resistance between the books, bat-

teries, center structure, and the inside layer of the multilayer insulation. This was done by first determining the black-body exchange coefficients, "*FA*," using an available computer program, "CONFAC II," then converting these to gray-body exchange coefficients, "Script *FA*," and multiplying by the cubic $M_{ij} = (T_i^2 + T_j^2)(T_i + T_j)$, which is obtained from factoring $T_i - T_j$ from $T_i^4 - T_j^4$. The procedure is as follows:

Since

$$R = \frac{\Delta T}{Q} ,$$

and

$$Q = \sigma \mathcal{F} A (T_1^4 - T_2^4) ,$$

then

$$R = \frac{1}{\sigma \mathcal{F} A (T_1^2 + T_2^2)(T_1 + T_2)} ,$$

where Q = heat flow
R = thermal resistance
σ = Stefan-Boltzmann constant
T_1, T_2 = absolute temperatures of the areas in question, and

$$\mathcal{F} A = \frac{1}{\frac{1}{A_1}\left(\frac{1}{\epsilon_1} - 1\right) = \frac{1}{FA} + \frac{1}{A_2}\left(\frac{1}{\epsilon_2} - 1\right)} ,$$

where A_1 = area at temperature T_1
A_2 = area at temperature T_2
ϵ_1 = infrared emissivity of A_1
ϵ_2 = infrared emissivity of A_2, and

$$FA = \iint_{A_1} \iint_{A_2} \frac{\cos \lambda_1 \cos \lambda_2 dA_1 dA_2}{\ell_{12}^2} ,$$

where ℓ_{12} = line connecting dA_1 and dA_2
λ_1 = angle between ℓ_{12} and the normal to dA_1
λ_2 = angle between ℓ_{12} and the normal to dA_2.

Another approach was needed for the radiation resistance through the insulation to the shell. Because of the many holes in the multilayer insulation, it was not possible to calculate the resistance through it more closely than an order of magnitude. Vacuum thermal testing was used to determine the value of the combined conduction and radiation resistance as a function of depth of insulation.

The combined radiation and conduction paths are shown in Fig. 3. For a first trial it is possible to treat radiation and conduction resistances in the same manner. To avoid unwieldly numbers in Fig. 3, the radiation resistances that are shown use the parameter $M = M_{ij} \times 10^{-6}$. This procedure allows the radiation paths to be treated as conductive paths with a correction of ΔM_{ij} when the temperatures change by ΔT_i or ΔT_j.

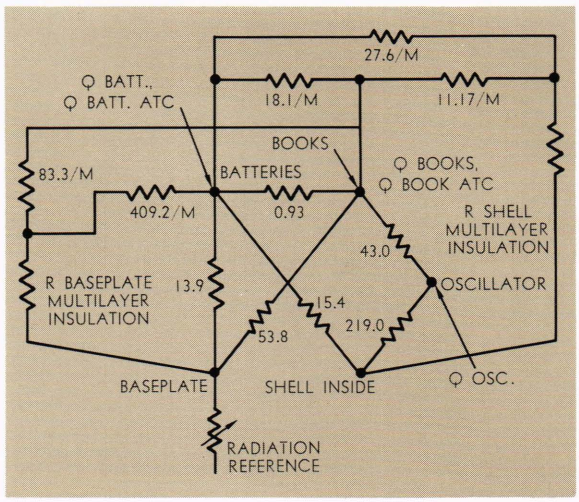

Fig. 3—Combined radiation and conduction paths.

Exterior Thermal Design and Thermal Coatings

The exterior of the satellite is composed of three general areas: I (shell), II (baseplate), and III (solar blades). The temperatures of these three areas are a function of the conduction and radiation resistances between them, as well as the external direct solar, earth-reflected solar, and earth-emitted energy rates, and the internally dissipated power of the satellite. The temperature of each area is that temperature at which the emitted energy rate of the area equals the input energy rate to that area.

The three steady-state temperatures of these regions are obtained from the three simultaneous equations generated by considering the shell, baseplate, and solar blades as closed systems.

AREA I (SHELL)—The heat input to the shell will be the sum of the radiation from solar blades to shell, conduction from solar blades to shell, conduction from baseplate to shell, absorbed solar energy, absorbed earth-reflected solar energy, and absorbed earth-emitted infrared radiation. This can be expressed mathematically as

$$Q_{in} = (K_R)_{SB\text{-}SH}(T_{SB}^4 - T_{SH}^4) + (K_C)_{SB\text{-}SH}(T_{SB} - T_{SH}) + (K_C)_{BP\text{-}SH}(T_{BP} - T_{SH}) + G_S \sum_n PAS_n \alpha_n + reG_S \sum_n F_{rese} A_n \alpha_n + (K_R)_{E\text{-}SH}(T_E^4 - T_{SH})^4$$

On the other hand, the heat output can only be the radiation from the shell to free space:

$$Q_{out} = (K_R)_{SH\text{-}SP}(T_{SH}{}^4 - 0),$$

which at equilibrium will equal the heat input.

AREA II (BASEPLATE)—The thermal input to the baseplate will be the sum of the internal satellite heating, the solar energy absorption, and the heating caused by absorption of earth-reflected sunlight:

$$Q_{in} = I.P. + G_S\alpha_{BP}PAS_{BP} + reG_S\alpha_{BP}\sum_m F_{rese}A_m .$$

The heat leaving the baseplate will be the sum of the energy conducted from baseplate to shell, radiation to space, and radiation to the earth:

$$\begin{aligned} Q_{out} = {} & (K_C)_{BP\text{-}SH}(T_{BP} - T_{SH}) + \\ & (K_R)_{BP\text{-}SH}(T_{BP}{}^4 - 0) + \\ & (K_R)_{BP\text{-}E}(T_{BP}{}^4 - T_E{}^4) , \end{aligned}$$

which at equilibrium will be equal to the heat input.

AREA III (SOLAR BLADES)—Heat input to the solar blades will be the sum of the heat absorbed from the sun and the absorbed earth-reflected sunlight:

$$Q_{in} = G_S\alpha_{SB}PAS_{SB} + reG_S\alpha_{SB}\sum_r F_{rese}A_r .$$

The heat output from the solar blades will be the sum of the infrared radiation to the earth, the heat conduction to the shell, infrared radiation to the shell, and radiation to space:

$$\begin{aligned} Q_{out} = {} & (K_R)_{SB\text{-}E}(T_{SB}{}^4 - T_E{}^4) + \\ & (K_C)_{SB\text{-}SH}(T_{SB} - T_{SH}) + \\ & (K_R)_{SB\text{-}SH}(T_{SB}{}^4 - T_{SH}{}^4) + \\ & (K_R)_{SB\text{-}SP}(T_{SB}{}^4 - 0) , \end{aligned}$$

and at equilibrium will be equal to the heat input.

Term definitions for the foregoing equations are:

(K_R) = Coefficient of radiation heat transfer
(K_C) = Coefficient of conductive heat transfer
$(I.P.)$ = Internal satellite power which is dissipated through the baseplate
PAS = Projected area to the sun
re = Earth's albedo (percent of incident solar power which is reflected by the earth)
F_{rese} = View factor of a satellite panel to the sunlit portion of the earth
T = Temperature in degrees R
Q = Heat flow
A = Area
G_S = Solar constant
α = Percent of incident solar energy rate which is absorbed.

Subscripts:

R = Radiation
C = Conduction
E = Earth
BP = Baseplate
SH = Shell
SB = Solar blades
SP = Space.

There is no direct radiation or conduction coupling between the solar blades and the baseplate. The net radiation and conduction between baseplate and shell is accounted for in the term containing the experimentally determined $(K_C)_{BP\text{-}SH}$.

There is no way to solve these equations for T_{SH}, T_{BP}, and T_{SB} without involving as many as 15 nonphysical solutions containing imaginary and negative absolute temperatures for each. An iteration process can be used to obtain the solutions to the desired accuracy.

If we let

$$\begin{aligned} T_{SH} &= Tx_o + x_o \\ T_{BP} &= Ty_o + y_o \\ T_{SB} &= Tz_o + z_o , \end{aligned}$$

then

$$\begin{aligned} T_{SH}{}^4 &\approx Tx_o{}^4 + 4Tx_o{}^3x_o \\ T_{BP}{}^4 &\approx Ty_o{}^4 + 4Ty_o{}^3y_o \\ T_{SB}{}^4 &\approx Tz_o{}^4 + 4Tz_o{}^3z_o . \end{aligned}$$

These approximations are substituted in Areas I, II, and III to form three new simultaneous linear equations in x_o, y_o, and z_o. Initial values of Tx_o, Ty_o, and Tz_o are assumed, and the appropriate projected area to the sun (PAS) values for the orbital position under consideration and appropriate values of $\alpha_{n,m,r}$ are substituted for the paint pattern under consideration, in this case all white. Values of x_o, y_o, and z_o are then calculated, and new values of T_x, T_y, and T_z are obtained:

$$Tx_1 = Tx_o + x_o;\ Ty_1 = Ty_o + y_o;\ Tz_1 = Tz_o + z_o.$$

The following substitutions are made:

$$Tx_o \rightarrow Tx_1;\ Ty_o \rightarrow Ty_1;\ Tz_o \rightarrow Tz_1;\ x_o \rightarrow x_1;\ y_o \rightarrow y_1;\ z_o \rightarrow z_1.$$

These are used to solve for x_1, y_1, and z_1. This process converges to x_n, y_n, $z_n < 0.5°$F very rapidly provided that suitable values are chosen for Tx_o, y_o, and z_o.

System Analog and Thermal Mock-up

The thermal resistances shown in Fig. 3 are

then put on an electrical analog device using the following analogy:

Current (10 ma) → (1.0 watt heat flow)
Potential Difference (100 mv) → 1°F
Resistance (10 ohms) → 1°F/watt.

The electrical analog device consisted of constant voltage power supplies to maintain voltage levels corresponding to calculated temperatures at the shell and baseplate reference nodes; constant-current power supplies to supply current at the book, battery, and oscillator nodes corresponding to the heat inputs at these points; and decade resistors with a resistance proportional to the thermal resistances between nodes.

As was discussed above, four thermal resistances could not be obtained analytically. Consequently, various calculated shell and baseplate temperatures were set on a thermal mock-up of the satellite in thermal vacuum tests. The heat inputs to the batteries, books, and oscillators were recorded along with their temperatures. This information was used to determine the thermal resistance through the multilayer insulation to the shell and baseplate, the resistance across the shell, and the resistance between shell inside and baseplate.

Prior to the thermal mock-up thermal vacuum tests, with these resistances unknown, it was not possible to know exactly how much of the power dissipated by books, batteries, and oscillator went to the shell and how much went to the baseplate. The steady-state temperatures of the shell and baseplate are proportional to the fourth root of the total heat flow, Q, into the node (internal plus external) and are inversely proportional to the fourth root of the area of the shell or baseplate.

The shell area is so large that the change in shell temperature per watt of internal dissipation is less than 1°F and can be neglected. However, the change in baseplate temperature per watt of internal dissipation is of the order of 3° to 5°F. Neglecting changes in baseplate temperature causes predicted internal temperatures to be notably lower than orbital results. The change in baseplate temperature is accounted for in the analog (Fig. 3) by setting up a baseplate reference and assuming a resistance between it and the baseplate. The value of this resistor is set to correspond to 1°F/watt. When the baseplate reference is set to a potential corresponding to the baseplate temperature assuming no dissipation of internal power, the current from books, batteries, and oscillator (corresponding to heat flow) which passes through the baseplate node to the baseplate reference node causes a potential difference between these nodes. This potential difference corresponds to the temperature increase in the baseplate caused by internal power dissipation, and therefore the baseplate potential corresponds to the actual baseplate temperature.

With this model the temperatures of the internal nodes were established over the range of conditions expected in orbit. It was then possible to evaluate temperature dependence in the radiation resistances with the relationship,

$$M_{ij} = (T_i^2 + T_j^2)(T_i + T_j) .$$

Book-to-battery resistances and baseplate reference-to-baseplate resistances were found to vary with temperature as given in Fig. 4. All other resistances were found to be reasonably insensitive to temperature, and radiation resistances could therefore be added to conduction resistances. The final analog for the whole satellite was then completed as shown in Fig. 5.

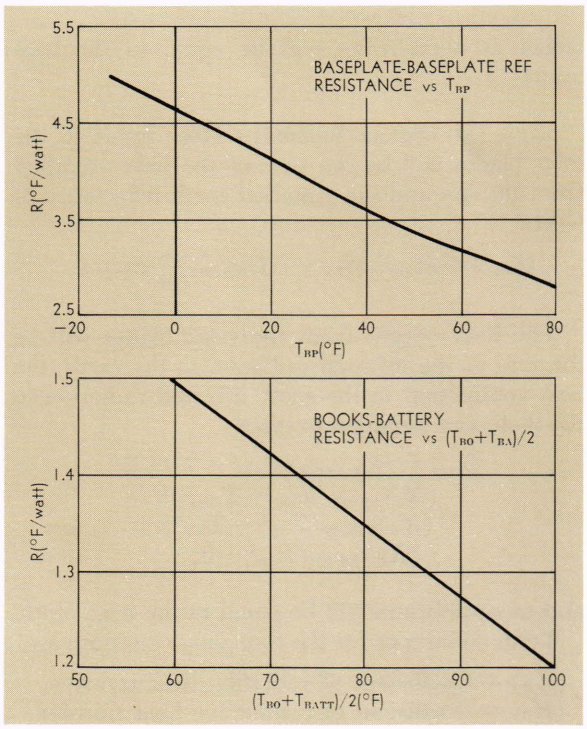

Fig. 4—Variable resistances for analog.

Conclusions and Results

The analog shown in Fig. 5 is capable of predicting book, battery, and oscillator temperatures to approximately ±1°F when compared to thermal vacuum test results. The only significant revision made to the analytically obtained analog for agreement with thermal vacuum test results was in the books-to-battery resistance. This lack of agreement is attributed to poor conductance through the joints

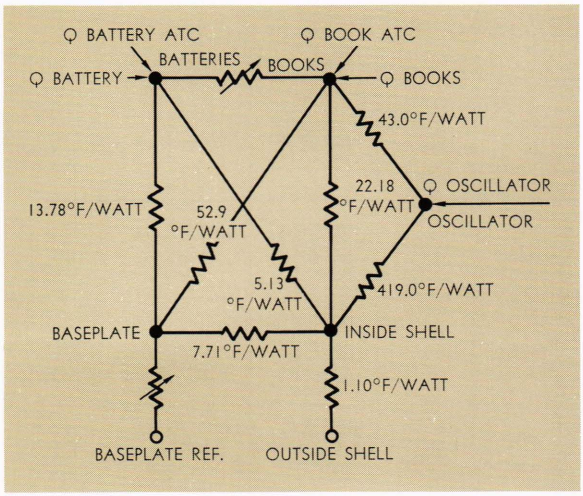

Fig. 5—Final flight hardware analog.

between individual books and to the complicated heat paths through the books. All other changes in the analog were negligible.

Having a good mathematical model (the analog), it was possible to determine the effect on temperature of variations in orbit which were unanticipated before launch; it was possible to see what changes if any were required in the satellite to meet the design goals; and it was possible to anticipate the effect on temperature and on the requirements for automatic temperature control power of changes in design of components in future satellites.

The predicted temperatures of the satellite under various orbital conditions are shown in Table I. For comparison purposes, the orbital temperatures for the baseplate and batteries are shown in Fig. 6 and for the oscillator and books in Fig. 7. Baseplate temperatures are almost entirely within the calculated range. The oscillator orbital temperatures are almost exactly equal to the thermal vacuum values, but the expected increase caused by seasonal variations in the solar constant failed to materialize. The predicted oscillator temperatures are therefore approximately 2½°F too high. The book temperatures are approximately 1½° to 2°F higher than the predicted values while the battery temperatures are approximately ½°F too high.

On the first satellite built to this design, orbital telemetry has indicated that almost all available automatic temperature control power was used shortly after launch during the random tumble phase while maintaining the batteries at 67°F. Later, as the satellite made the transition to an orbital configuration such that the satellite was never in the earth's shadow throughout the orbit, the automatic temperature control power approached zero while the battery temperature rose to 72°F. This indicates that the automatic temperature devices are functioning as designed.

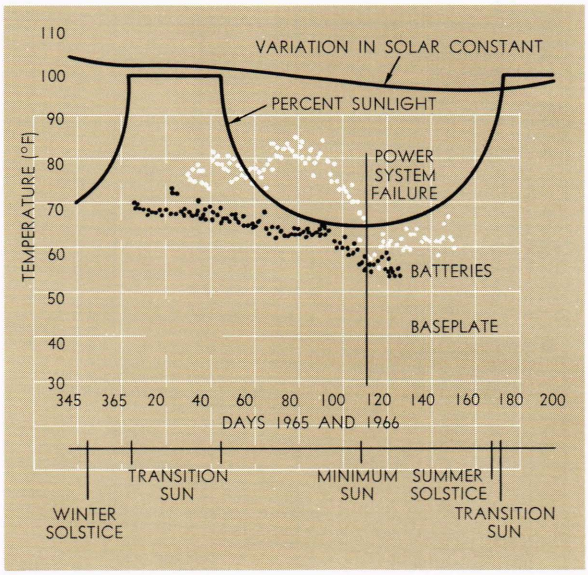

Fig. 6—Comparison of predicted and orbital temperatures for baseplate and batteries.

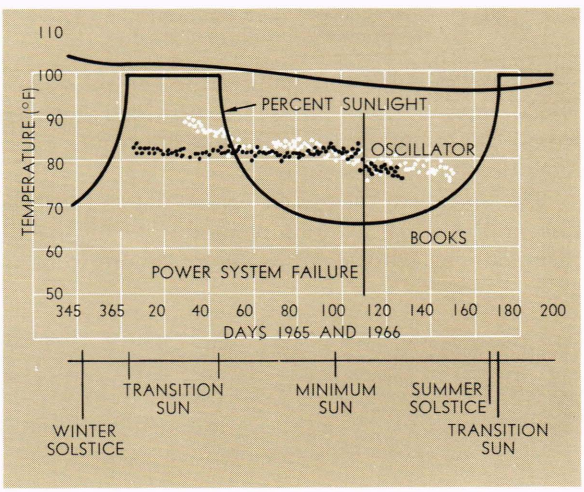

Fig. 7—Comparison of predicted and orbital temperatures for oscillator and books.

The second and third satellites built to this design agree with the first within approximately 2°F, indicating that the design is basically stable and very reproducible and therefore requires no individual tailoring.

The use of 16 individual heaters will greatly in-

TABLE I

PREDICTED TEMPERATURES OF SATELLITE UNDER VARIOUS ORBITAL CONDITIONS

Case	*Nominal*		*Coldest**		*Hottest**		*Books**	*Batteries**	*Oscillator**
	Shell	*Base-plate*	*Shell*	*Base-plate*	*Shell*	*Base-plate*			
Minimum Sun, Magnetic	−30°	+31°	−34°	+23°	−24°	+39°	67° Avg. 66–68~ (±1°F)	62.5° Avg. 59–66~ (±2°F)	80° (±5°)
Minimum Sun, Gravity, Initial Time	−32°	+36°	−36°	+28°	−26°	+44°	67° Avg. 66–68~ (±1°F)	64.5° Avg. 61–68~ (±2°F)	81° (±5°)
Gravity, Transition Sun, Initial-Time	−19°	+45°	−22°	+33°	−13°	+56°	69° Avg. 68.5–69.5~ (±1°F)	68° Avg. 67–69~ (±1°F)	83° (±3°)
Minimum Sun, Gravity, One-Year Degradation	−21°	+48°	−25°	+40°	−15°	+56°	69.5° Avg. 68.5–70.5~ (±1.5°F)	66.5° Avg. 63–70~ (±1°F)	83° (±2°)
Transition Sun, One-Year Degradation	− 3°	+67°	− 6°	+59°	+ 3°	+75°	71.0° Avg. 70.5–71.5~ (±1.0°F)	69.2° Avg. 68–70~ (±1.5°F)	86° (±1°)
Launch, Spin Stabilized	Shell −10° to +30°, Rad. 10°–80°						60–90°	55–85°	70–105°

* The coldest and hottest case conditions account for maximum effects of variations of the solar constant from 429.3 to 459.0 btu/hr-ft², and the maximum effect of a 10° (0 to peak) libration averaged over the orbit. The (± × °F) figures under books, batteries, and oscillator are the predicted results of this effect.

crease reliability of the temperature control system. Good heat transfer paths are provided between components, and failure of one heater will be compensated for by adjacent units.

The so-called "degraded" cases tested (darkening of the white exterior paint due to ultraviolet degradation) correspond to the maximum value of degradation expected in one year. Consequently, the satellite books and batteries will probably be maintained at temperatures in the range of 65° to 75°F for several years. The nearly constant book and battery temperature will also extend the life of the satellite's memory and power system and should provide an overall long life for the satellite.

PUBLICATIONS

The following list is a compilation of recently published technical articles written by APL staff members.

M. H. Friedman, "Shock Tube Measurement of Explosive Sensitivity," *Combustion and Flame,* **10,** No. 2, June 1966, 112-119.

M. H. Friedman, "Approximate Closed Solutions for Detonation Parameters in Condensed Explosives," *AIAA J.,* **4,** No. 7, July 1966, 1182-1187.

S. M. Yionoulis, "Determination of Coefficients Associated with the Geopotential Harmonic of Degree and Order (n,m) = (13, 12)," *J. Geophys. Res.,* **71,** No. 16, Aug. 15, 1966, 4064.

V. G. Sigillito, "Pointwise Bounds for Solutions of the First Initial-Boundary Value Problem for Parabolic Equations." *Soc. Ind. Appl. Math., J. Appl. Math.,* **14,** No. 5, Sept. 1966, 1038-1056.

R. M. Hanes and J. W. Gebhard, "The Computer's Role in Command Decision," *U.S. Naval Inst. Proc.,* Sept. 1966, 60-68.

L. Monchick (APL), R. J. Munn (University of Belfast, Ireland), and E. A. Mason (University of Maryland), "Thermal Diffusion in Polyatomic Gases: A Generalized Stefan-Maxwell Diffusion Equation," *J. Chem. Phys.,* **45,** No. 8, Oct. 15, 1966, 3051-3058.